Molecular Immunology 187 (2025) 152–165

Contents lists available at ScienceDirect

Molecular Immunology

journal homepage: www.elsevier.com/locate/molimm

Protocatechuic aldehyde promotes diabetic wound healing by enhancing angiogenesis via H3K18 lactylation-mediated Acvr1c expression

Weijing Fan [1], Yang You [1], Yin Qu [*], Guobin Liu [*]

Shuguang Hospital Affiliated to Shanghai University of Traditional Chinese Medicine, Shanghai 201203, China

ARTICLE INFO

Keywords:
Protocatechuic aldehyde
H3K18 lactylation
wound healing
diabetes mellitus

ABSTRACT

Delayed wound recovery is a major health issue affecting people with diabetes. Histone lactylation is involved in tissue repair. However, it is not clear whether protocatechuic aldehyde (PCA) promotes diabetic wound healing through histone lactylation. In this study, a diabetic wound mouse model was constructed to delve into the role of PCA in vivo. Chromatin immunoprecipitation sequencing (ChIP-seq) was used to determine genes affected by H3K18 lactylation (H3K18la) under PCA treatment. The effects and mechanisms of PCA on histone lactylation and angiogenesis were investigated through cellular experiments. We found that PCA accelerated wound healing and angiogenesis in diabetic mice, and significantly reduced the inflammatory response in wound tissues. Lactate and H3K18la levels were augmented in the model group in comparison with the control group, however, PCA treatment remarkably reversed their levels. ChIP-seq analysis revealed a significant enrichment of H3K18la at the Acvr1c locus, and this histone modification was downregulated by PCA treatment. PCA remarkably enhanced Acvr1c expression through H3K18la in HUVECs. Moreover, PCA treatment markedly elevated cell viability, migration and tube formation in comparison with the control group. However, this effect was counteracted by Acvr1c knockdown. In conclusion, PCA promoted HUVEC angiogenesis by increasing H3K18la-mediated Acvr1c expression, thereby promoting diabetic wound healing. This could offer a new treatment approach to enhance the effectiveness of healing diabetic wounds.

1. Introduction

Diabetes mellitus is a progressively widespread chronic endocrine disorder marked by sustained high blood sugar levels (Defeudis et al., 2022). The growing incidence of diabetes on a global scale has transformed it into a significant worldwide health challenge (Zheng et al., 2018). An estimate shows that one-third to one-fifth of diabetes patients will experience chronic non-healing wounds, such as diabetic foot ulcers, during their lifetime, with a staggering recurrence rate of 40 % within one year and 65 % within five years, and there are no dependable ways to forecast their occurrence (Burgess et al., 2021; Chang and Nguyen, 2021). Wound healing is influenced by a variety of factors, such as skin damage, diabetic neuropathy, angiogenesis, infection, and poor blood sugar control (Deng et al., 2021; Okonkwo and DiPietro, 2017). Among these factors, angiogenesis serves as a critical modulator, leading to the supply of nutrients and oxygen to the wound areas (Wang et al., 2024). However, there is still a lack of comprehensive understanding of the mechanisms regulating endothelial cell angiogenesis in diabetic wound healing.

Protocatechuic aldehyde (PCA) is a phenolic substance naturally present in the Chinese medicine Danshen. Previous research has shown that PCA exhibits anti-inflammatory, and antioxidant properties (Kim et al., 2008; Wei et al., 2013). PCA has been proven to play a therapeutic role in a variety of diseases. PCA reduceed cisplatin-triggered acute renal damage by inhibiting Nox-dependent oxidative stress and inflammation (Gao et al., 2016). PCA alleviated isoproterenol-mediated cardiac hypertrophy by blocking the JAK2/STAT3 axis (Fang et al., 2018). However, there have been no reports on the role of PCA in

Abbreviations: PCA, protocatechuic aldehyde; ChIP-seq, Chromatin immunoprecipitation sequencing; H3K18la, H3K18 lactylation; HUVECs, human umbilical vein endothelial cells; H&E, hematoxylin and eosin; GO, Gene Ontology; KEGG, Kyoto Encyclopedia of Genes and Genomes; DMEM, Dulbecco's Modified Eagle Medium; FBS, fetal bovine serum; HG, high glucose; CCK-8, Cell counting kit-8; QRT-PCR, quantitative real-time PCR; SD, standard deviation; ANOVA, analysis of variance.

* Correspondence to: No. 528 Zhang Heng Road, Pudong New Area, Shanghai, China.
E-mail addresses: quyin2004@163.com (Y. Qu), 15800885533@163.com (G. Liu).
[1] Co-first author

https://doi.org/10.1016/j.molimm.2025.09.002
Received 18 April 2025; Received in revised form 27 August 2025; Accepted 10 September 2025
Available online 30 September 2025

diabetic wound healing.

Histone lactylation has emerged as a new type of histone post-translational modification that connects cellular metabolism with epigenetic modulation (Zhang et al., 2019). Histone lactylation is engaged in the development of multiple diseases, including cancer, cardiovascular diseases, and diabetes (Huang et al., 2024; Lin and Ren, 2024; Xie et al., 2022). Lactate elevated the level of histone H3 lysine 14 lactylation in diabetic kidney disease and histone lactylation promoted epithelial-mesenchymal transition (Zhang et al., 2024). In diabetic retinopathy, histone lactylation upregulated FTO expression, thereby aggravating microvascular abnormalities (Chen et al., 2024). H4K12 lactylation amplified mitochondrial oxidative stress through the FoxO1 pathway, thereby exacerbating diabetes-related cognitive impairment (Yang et al., 2025). Nevertheless, the function of lactylation modification in diabetic wound healing remains unexplored. The involvement of PCA in diabetic wound healing via lactylation modification is yet to be determined.

In this study, we aim to delve into the role and related mechanisms of PCA in diabetic wound healing. To accomplish this objective, PCA was applied in a diabetic mouse model with skin wounds and in human umbilical vein endothelial cells (HUVECs). Chromatin immunoprecipitation sequencing (ChIP-seq) was applied to screen genes exhibited histone lactylation modification and involved in diabetic wound healing. A series of cellular experiments were conducted to explore the role of key genes in angiogenesis. This study provides a new therapeutic approach for diabetic wound healing.

2. Material and methods

2.1. Sample collection

Non-diabetic control skin tissues from three cases without diabetes who underwent acute trauma surgery due to foot injury, and foot wound tissues from five diabetes mellitus patients were collected. All participants provided written informed consent. This study was authorized by the Ethics Committee of Shuguang Hospital Affiliated to Shanghai University of Traditional Chinese Medicine.

2.2. Diabetic Skin wound mouse model

A total of 6 male C57BL/6 J mice and 12 male C57BL/KsJ db/db mice, each weighing 20 ± 2 g and aged 8 weeks, were sourced from SPF Biotechnology Co., Ltd. (China). The mice were housed under conditions of 24°C ± 1°C, 50 ± 5 % humidity, and a 12-hour light-dark cycle. They had unrestricted access to food and water. All experiments were approved by the Ethical Committee of Shuguang Hospital Affiliated to Shanghai University of Traditional Chinese Medicine.

The animal experiment was designed with three groups (n = 6 each): wild-type normal (control) group, db/db (model) group, and model+PCA group. Prior to the surgical procedure, all mice were anesthetized with 50 mg/kg of pentobarbital sodium. Following hair removal and sterilization, a 6 mm full-thickness wound was created on the dorsal surface of each mouse. The mice in the PCA group were given 35 mg/kg PCA gavage daily according to the research of Ji et al. (2021) with some modification. Photographs were captured on Days 0, 3, 7,10, and 14 to measure the wound area. ImageJ software was employed to process the samples on Days 0, 3, 7,10, and 14, with the healing rate quantified as the percentage of the initial wound area. On the 14th day following the induction of wounds, the weight, glucose and HbA1c was detected, and wound tissues were harvested for subsequent research.

2.3. Histological analysis

The wound tissues were fixed in 4 % paraformaldehyde solution. Following the processes of dehydration and embedding, the tissue was converted into wax blocks and loaded onto a microtome for slicing at a thickness of 4 μm. The paraffin-embedded sections were then subjected to dewaxing in water, followed by hematoxylin and eosin (H&E) staining and Masson's trichrome staining. After dehydration, the sections were mounted on glass slides and examined with a microscope.

2.4. Immunofluorescence

Skin tissues were preserved using 4 % paraformaldehyde, then embedded in paraffin and cut into sections. Sections of 4 μm in thickness underwent antigen retrieval and were treated with 0.5 % Triton X-100 for permeabilization. Following this, the slides were blocked with 5 % BSA for one hour at room temperature. The slides were probed with primary antibody against iNOS (22226–1-AP, Proteintech), CD206 (18704–1-AP, Proteintech), CD31 (28083–1-AP, Proteintech), CD146 (17564–1-AP, Proteintech), H3K18la (PTM-1406RM, PTMBIO) and Acvr1c (67417–1-Ig, Proteintech) overnight at 4°C and then with a secondary antibody Goat Anti-Rabbit IgG H&L (Alexa Fluor® 488) (ab150077, Abcam) for one hour at room temperature. Nuclei were counterstained with DAPI. Imaging was conducted using an inverted fluorescence microscope (OLYPUS, CKX53).

2.5. Lactate content detection

The lactic acid assay kit (Sangon Biotech, D799099–0100) was employed to measure lactate levels in skin and blood of mice. Samples were mixed with extraction reagent 1, after which they were subjected to centrifugation at 4°C and 12,000 g for a duration of 10 min. Subsequently, extraction reagent 2 was added to the resultant supernatant, which was then recentrifuged at 12,000 g for another 10 min. The lactate concentration was determined at 570 nm with a spectrophotometer (Thermo Fisher).

2.6. ATP detection

ATP levels were measured with an ATP assay kit (Shanghai Tongwei Biotechnology Co., LTD, China) in strict accordance with the protocol provided by the manufacturer.

2.7. ChIP-seq

Skin tissue samples from the model group and the treatment group mice were used for ChIP-seq. ChIP-seq was carried out at the laboratory of MivectorBio Co., Ltd. by experienced research personnel. DNA fragments that specifically associate with the target proteins were selectively enriched through the use of the H3K18la antibody (PTMBIO, PTM-1427RM). Following enrichment, these DNA fragments were meticulously purified to prepare them for the next steps. The purified DNA fragments were then employed to assemble comprehensive sequencing libraries. These libraries were subsequently analyzed by sequencing on the Illumina Novaseq X 10B platform.

The raw sequencing data were processed to remove adapters and underwent quality control to obtain clean reads for subsequent data analysis. The filtered clean reads were aligned to the reference genome of the corresponding species using the Bowtie2 software to obtain unique mapped reads. The macs2 software was employed for the identification of Peak Calling and their annotation analysis, aimed at pinpointing regions of histone lactylation and elucidating the distribution patterns of these peaks across various genomic elements. Subsequently, the MEME software was utilized to conduct motif analysis on the identified peaks. The MAnorm2 software is used to reveal the dynamic changes of histone modifications. Genes with differential expression are subjected to Gene Ontology (GO) and Kyoto Encyclopedia of Genes and Genomes (KEGG) analysis.

2.8. Cell culture and treatment

HUVECs were acquired from iCell. The cells were grown in Dulbecco's Modified Eagle Medium (DMEM) supplemented with 10 % fetal bovine serum (FBS) in an incubator set to 37 °C with a 5 % CO2 environment. To probe into the impacts of high glucose (HG) and PCA on endothelial cell function, we treated HUVEC cells with 0 and 50 mM HG for 72 h, and then exposed them to various concentrations of PCA (0.72–72.46 μM) for 24 h.

2.9. Cell transfection

Acvr1c siRNAs and si-NC were acquired from GenePharma (Shanghai, China). To transfect the Acvr1c siRNAs and si-NC into HUVECs, the Lipofectamine 2000 reagent kit (Invitrogen, USA) was utilized, following the protocol provided by the supplier.

2.10. Cell counting kit-8 (CCK-8)

The cellular proliferation capacity was assessed using the CCK-8 (Beyotime). The cell density was diluted to 10^4 cells/ml in complete medium, after which 100 μL of the prepared suspension was dispensed into each well of a 96-well plate. Subsequently, cells were treated with different reagents according to different experimental purposes. HG treatment was conducted by treating HUVECs with 50 mM glucose. Controls (NC) were conducted by treating HUVECs with 5.5 mM glucose. To determine the optimal usage concentration of PCA in HUVECs treated with HG, HUVECs were treated with 0 μM, 0.72 μM, 1.45 μM, 3.62 μM, 7.25 μM, 14.49 μM, 28.99 μM, 43.48 μM, 57.97 μM and 72.46 μM PCA for 24 h. To clarify that the observed effect was caused by HG itself rather than osmotic stress, mannitol (50 mM) was used as a control of osmotic stress (Tousian et al., 2020). To explore the effect of Acvr1c knockdown on the proliferation of HUVECs treated with PCA, HUVECs were divided into 4 groups: HG, HG+PCA, HG+recombinant human basic fibroblast growth factor (rh-bFGF, 50 ng/ml), and HG+PCA+si-Acvr1c groups. The usage concentration of rh-bFGF referred to the literature of Zhang et al. (2022). Prior to the assay, 10 μl of CCK-8 solution was introduced into each well and incubated at 37 °C for a period of 1 h. Absorbance at 450 nm for each well was then recorded with a microplate reader (Infinite M1000, TECAN).

2.11. ChIP-qPCR

ChIP assays were conducted using the ChIP kit (Millipore). In summary, 2×10^7 cells were fixed with 1 % formaldehyde, after which excess formaldehyde was neutralized by adding 1 ml of 2.5 M glycine. The cells were then subjected to lysis with a specific buffer. Genomic DNA was fragmented into smaller pieces via sonication. Antibodies H3K18la (PTMBIO, PTM-1427RM) were employed to immunoprecipitate DNA fragments. An input sample served as a control. The enrichment of each DNA fragment was quantified using quantitative real-time PCR (qRT-PCR). The primer sequences are detailed in Table S1.

2.12. qRT-PCR

RNA extraction was executed using TRIzol reagent (Thermo, USA) as per the protocol provided by the manufacturer. Subsequently, the isolated RNA was converted into cDNA with the PrimeScript RT Master Mix (Thermo). Quantification of relative mRNA expression was conducted via SYBR Green PCR Master Mix (Roche) on an ABI Q6 system (Applied Biosystems Inc.USA), with calculations made by utilizing the $2^{-\Delta\Delta Ct}$ method. The primer sequences used are provided in Table S2.

2.13. Western blot

Cell and skin tissue samples were harvested and disrupted using RIPA lysis buffer. After protein separation by SDS-PAGE, they were transferred onto PVDF membranes. These membranes were then blocked with 5 % non-fat dry milk for 1.5 h, after which they were incubated overnight at 4 °C with primary antibodies against Acvr1c (1:3000, 67417–1-Ig, Proteintech), H3K18la (1:2000, PTM-1406RM, PTM-Biolab), H3K9la (1:2000, PTM-1419RM, PTM-Biolab), H4K12la (1:2000, PTM-1411RM, PTM-Biolab), Histone H3 (1:5000, 17168–1-AP, Proteintech), VEGFR2 (1:1000, 26415–1-AP, Proteintech), Hes1 (1:1000, ab71559, Abcam) and GAPDH (1:15000, 60004–1-lg, Proteintech). The membranes were next treated for one hour with HRP-conjugated secondary antibodies, including goat anti-mouse IgG H&L (1:5000, RGAM001, Proteintech) and goat anti-rabbit IgG H&L (1:5000, RGAR001, Proteintech). Protein band visualization was performed using an enhanced chemiluminescence kit, and the band intensities were quantified using ImageJ analysis software.

2.14. Dual-luciferase reporter assay

Wild-type or mutant 3′-UTR of Acvr1c (Acvr1c-WT or Acvr1c-MUT) fragments were amplified and cloned into pmirGLO vectors (Promega). 293 T cells were subjected to transfection with luciferase reporter plasmids using lipofectamine 2000 (Invitrogen). Luciferase activity was then determined in the resulting lysates using the Dual-Luciferase Reporter Assay System (Promega).

2.15. Wound healing assay

The migration capability of cells was assessed through a wound healing assay. Cells were seeded into 24-well plates and a new 200 μl pipette tip was used to pass through the center of the hole. Following a PBS wash to eliminate detached cell debris, the wounds were captured under an inverted microscope at 0 and 24-hour intervals. The wound closure was quantitatively analyzed by measuring the wound gap with Image J software.

2.16. Tube formation assay

To evaluate the role of Acvr1c knockdown on the tube formation ability of PCA-treated HUVECs, a tube formation assay was conducted. In brief, Matrigel (356230, Corning) was appended to a pre-chilled 24-well plate at 200 μl per well and put in a 37°C incubator for 1 h to allow it to solidify. HUVECs at a concentration of 1.5×10^5 cells per well were added to the plate. After 24 h, the formation of capillary-like structures was examined using an inverted phase contrast microscope (NIKON), and the structures were quantified using ImageJ software.

2.17. Statistical analysis

Statistical analysis was carried out using GraphPad Prism software (version 9.0.0) and data are reported as mean ± standard deviation (SD). To compare two groups, a Student's *t*-test was utilized. For analyses involving more than two groups, a one-way analysis of variance (ANOVA) followed by Tukey's post-hoc test was performed. A threshold of $P < 0.05$ was adopted as the criterion for statistical significance.

3. Results

3.1. PCA promotes diabetic wound healing

To investigate the effect of PCA on diabetic wound healing, PCA was administered to diabetic mice by gavage. Fig. 1A illustrated the process of diabetic wound healing after treatment with PCA at days 0, 3, 7, 10 and 14. Quantitative analysis revealed that the wound area in the model group was prominently larger than that in the control group, while PCA treatment remarkably diminished the wound area of the model mice (Fig. 1B). Consistently, mice in the model group exhibited significantly

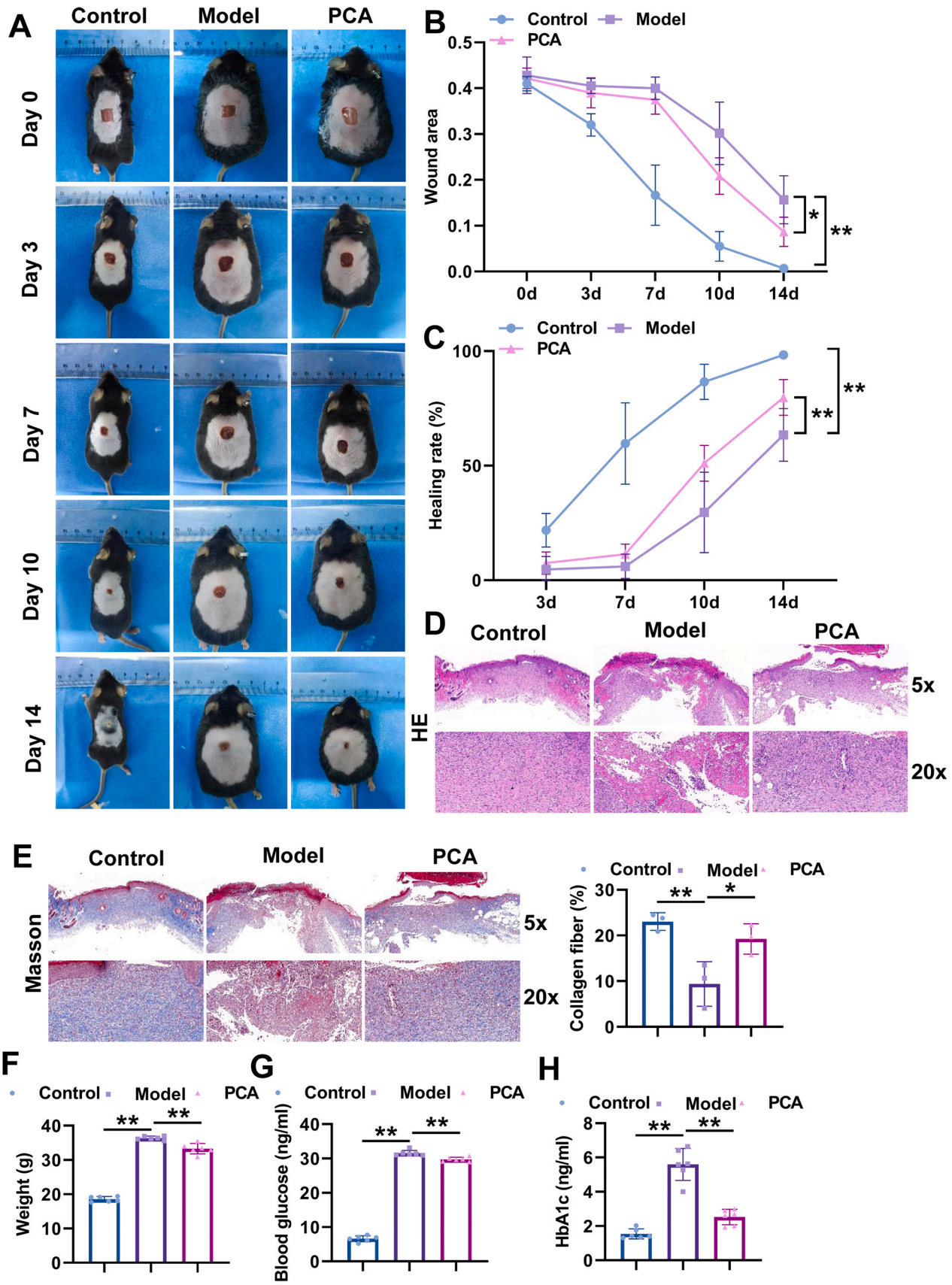

Fig. 1. Protocatechuic aldehyde (PCA) promotes diabetic wound healing. (A) Representative mages of the diabetic wounds in control, model, and PCA group at day 0, 3, 7, 10, and 14. (B) Wound area and (C) healing rate were measured at day 0, 3, 7, 10, and 14. HE (D) and Masson (E) staining of representative wounds in control, model, and PCA group. (F) The effect of PCA treatment on mice weight. (G) The effect of PCA treatment on mice blood glucose levels. (H) The effect of PCA treatment on HbA1c levels. n = 6. **p < 0.01, *p < 0.05.

decreased wound healing rate compared with the control group, whereas PCA treatment significantly augmented the wound healing rate of the model mice (Fig. 1C). H&E staining showed that the model group exhibited epithelial abnormalities and marked structural changes, accompanied by a significant inflammatory cell infiltration (Fig. 1D). PCA treatment could significantly reverse this unfavorable trend (Fig. 1D). Masson staining showed that PCA treatment alleviated the reduction of collagen deposition in the model mice (Fig. 1E). Moreover,

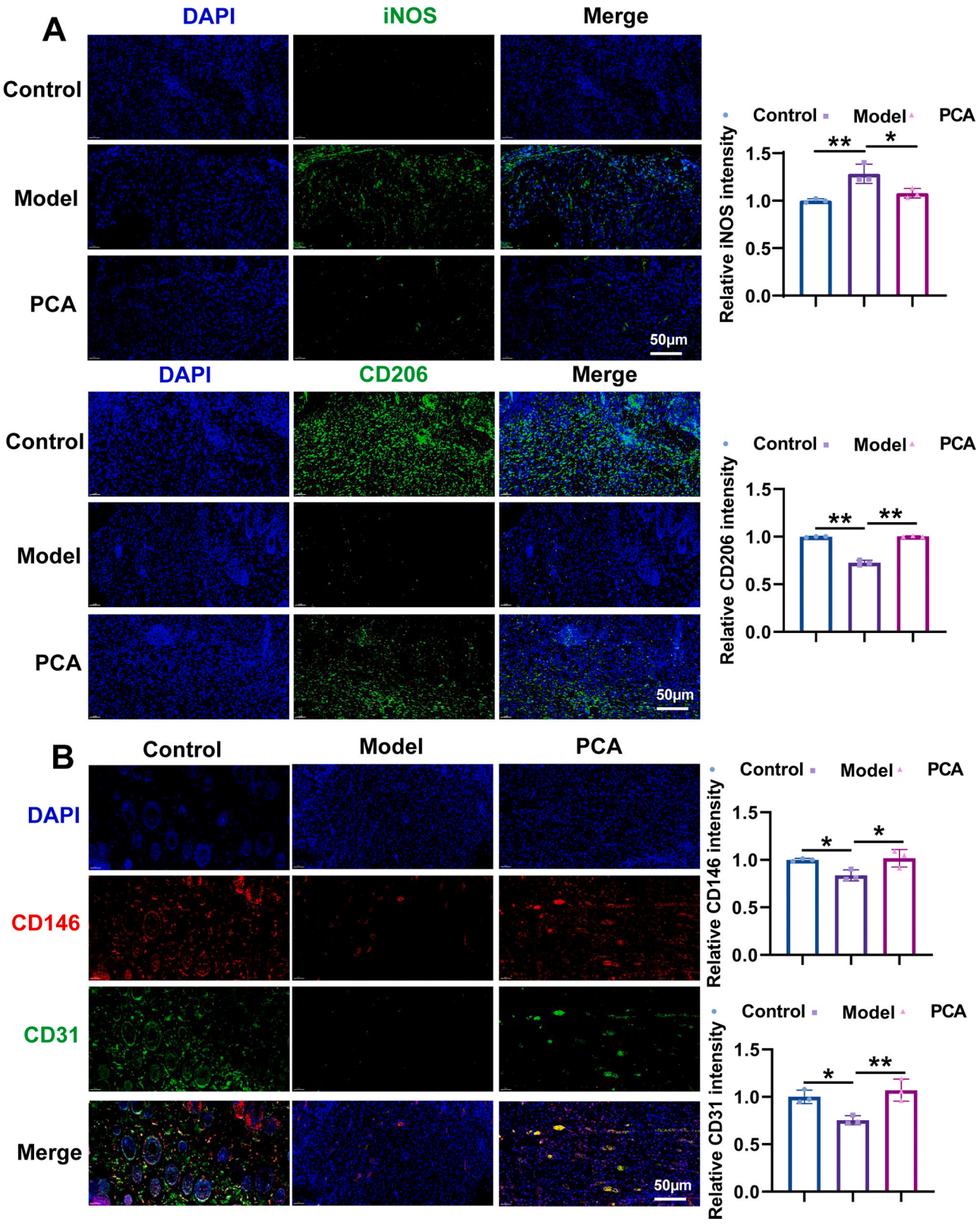

Fig. 2. PCA alleviates inflammation and promoted angiogenesis of model mice. (A) The expression of iNOS and CD206 in diabetic wound tissues was detected by immunofluorescence. (B) The expression of CD146 and CD31 in diabetic wound tissues was detected by immunofluorescence. **p < 0.01, *p < 0.05.

compared with the control group, the model group exhibited a significant increase in body weight, blood glucose levels, and HbA1c levels (Fig. 1F-H). However, treatment with PCA markedly reduced body weight, blood glucose, and HbA1c levels. Subsequently, immunofluorescence detection was used to assess the expression of iNOS and CD206 in the wound tissue to evaluate the inflammatory response. The results uncovered that the expression of iNOS was remarkably enhanced, CD206 was obviously decreased in the model group compared with the control group, whereas PCA treatment reversed this trend (Fig. 2A). The immunofluorescence co-staining for CD31 and CD146 revealed that compared to the control group, the expression of CD31 and CD146 was markedly decreased in the model group, while PCA treatment could reverse this trend, indicating that PCA treatment promoted angiogenesis of the diabetic mice (Fig. 2B). Collectively, these results indicated that PCA promoted diabetic wound healing.

3.2. PCA inhibits histone lactylation of endothelial cells in diabetic wound

To investigate whether histone lactylation was involved in PCA treatment, the lactic acid and ATP levels in the wound tissues of each group were measured. The results revealed that the lactic acid and ATP levels in the blood and skin of the model group were significantly higher than those in the control group, while PCA treatment could counteract this trend (Fig. 3A-D). We then analyzed the lactylation levels of a series of histone lactated residues, including H4K12la, H3K9la and H3K18la. There were no significant differences in H3K9la and H4K12la expression among the control, model, and PCA groups (Figs. 3E, 3G). In contrast, the model group exhibited a marked increase in H3K18la expression compared with the control group, whereas PCA treatment significantly reduced H3K18la expression (Figs. 3F, 3H), suggesting that PCA modulated histone lactylation at H3K18. Immunofluorescence co-staining for CD31 and H3K18la revealed that CD31 and H3K18la were co-localized, and H3K18la expression was remarkably enhanced in endothelial cells of the model group relative to the control group, whereas PCA diminished H3K18la expression in model mice (Fig. 3I). Overall, these data indicated that PCA suppressed histone lactylation of endothelial cells in diabetic wound.

3.3. PCA regulates modified landscape of histone lactylation

To investigate the mechanism of H3K18la in diabetic wound under PCA treatment, ChIP-seq was employed to explore genes modulated by H3K18la in skin tissues from the model and PCA groups. Genome mapping analysis revealed that in the model group, there were 63,782,754 raw reads, of which 27,980,770 were clean reads, with a mapping rate of 79.50 % to the reference genome (Table S3). The PCA group had 64,376,664 raw reads, comprising 30,184,654 clean reads, with a mapping rate of 76.11 % to the reference genome (Table S3). Analysis of peak annotation indicated that in both the model and PCA groups, the regions with histone lactylation were roughly 500 bp in width (Fig. 4A). In the model group, histone lactylation was predominantly found in distal intergenic regions (35.2 %), followed by promoter regions (34 %), and the 1st intron (6.01 %) (Fig. 4B). The PCA group showed a higher proportion of modifications in promoter regions (38.65 %), followed by distal intergenic regions (31.52 %) and the 1st intron (6.13 %). The heatmap showed that enrichment of peak was near the transcription start sites (Fig. 4C). Motif analysis showed that the prime motif in the model group was GAACTTAGGAAATTAGTCTGAACAGGTGAGAGGGTG, while the prime motif in the PCA group was AACTTAGGAAATTAGTCTGAACAGGTGAGAGGGTG (Fig. 4D). To delve deeper into the dynamic alterations of histone lactylation, we conducted a comparative analysis of the peak distribution between the model and PCA groups. The results revealed that 4487 upregulated peaks and 2079 downregulated peaks were identified in the PCA group relative to the model group (Figs. 5A, 5B). To investigate the function of H3K18la in diabetic wound following PCA treatment, GO and KEGG pathway analyses of genes exhibiting differential peaks were conducted. Notably, genes were enriched in multiple pathways related to angiogenesis, including wound healing, adherens junction, regulation of angiogenesis, Wnt, MAPK, Notch and TGF-beta signaling pathways (Figs. 5C, 5D). These results indicated that H3K18la binding genes was related with angiogenesis.

3.4. PCA inhibited H3K18la modification at the Acvr1c locus but upregulated Acvr1c expression

To study whether PCA regulated histone lactylation in vitro, we first treated HUVECs with 0 and 50 mM glucose and then exposed them to different concentrations of PCA (0.72–72.46 μM). CCK-8 results revealed that PCA at 0.72, 1.45 and 3.62 μM markedly improved cell viability of HG-treated HUVECs and 1.45 μM had the best promoting effect (Fig. 6A). Therefore, this concentration was chosen for the next study. As shown in Fig. 6B, PCA treatment at concentrations ranging from 0.72 μM to 28.99 μM significantly decreased lactic acid levels compared with the untreated group. Immunofluorescence showed that HG obviously increased H3K18la expression in HUVECs (Figs. 6C, 6D). Considering that H3K18la was downregulated in the PCA group, genes with downreguated H3K18la engaged in Hippo, TGF-beta, Notch, and Wnt signaling pathways (Fan et al., 2023; Huang et al., 2021; Liu et al., 2023), which were related with angiogenesis, were selected (Fig. 6E). Visualized analysis revealed the signal intensity of lactylation peaks of five candidate genes (Id2, Bmp7, Acvr1c, Hdac2, and Rbx1) in model and PCA groups (Fig. 6F). Subsequently, the ChIP-qPCR assay was utilized to examine the lactylation of these five genes. The results showed that in comparison with the model group, H3K18la of Acvr1c was remarkably decreased in the PCA group, whereas there were no significant differences in H3K18la of Id2, Bmp7, Hdac2, and Rbx1 (Fig. 6G-K). Therefore, Acvr1c was selected for the subsequent study. Dual-luciferase reporter assay showed that PCA significantly increased the luciferase activity of Acvr1c-WT, but did not affect Acvr1c-MUT (Fig. 6L). PCA treatment remarkably increased the mRNA expression of Acvr1c in the wound tissues of diabetic mice (Fig. 6M). qRT-PCR and western blot uncovered that HG significantly decreased the mRNA and protein expression of Acvr1c in HUVECs, while PCA enhanced the expression of Acvr1c in HG-treated HUVECs. However, this trend was reversed by lactic acid supplementation (Figs. 6N, 6O). In addition, we detected the expression of Acvr1c and H3K18la in control and diabetic wound tissues by immunofluorescence. The results showed that the expression of Acvr1c was significantly down-regulated in diabetic wound tissues, while the expression of H3K18la was significantly up-regulated (Figure S1A, B). Correlation analysis revealed a negative correlation between H3K18la and Acvr1c (Figure S1C). Together, PCA promoted Acvr1c expression through H3K18la.

3.5. PCA increases Acvr1c expression to promote endothelial angiogenesis

To investigate whether PCA regulated angiogenesis through Acvr1c, Acvr1c siRNAs were transfected into HUVECs. qRT-PCR results showed that si-Acvr1c-1 and si-Acvr1c-3 remarkably inhibited the Acvr1c mRNA expression, with si-Acvr1c-1 achieving the best effect (Fig. 7A). This result was further verified by western blot (Fig. 7B). To explore the regulation of Acvr1c on the VEGF/Notch pathway, we detected the expressions of VEGFR2 and Hes1 in HUVECs with Acvr1c knockdown via western blot. The results showed that Acvr1c knockdown significantly reduced VEGFR2 and Hes1 expression (Fig. 7C). To enhance the claim that the effect of PCA is caused by HG, we use mannitol as a control for osmotic stress. The CCK-8 results showed that PCA could reverse the inhibitory effect of HG on the proliferation of HUVECs, while mannitol had no significant effect on the proliferation of HUVECs (Fig. 7D). We then explored the effects of PCA and Acvr1c knockdown on HUVEC angiogenesis. In the CCK-8 assay, the PCA group demonstrated a markedly elevated cell viability compared to the HG group, which was

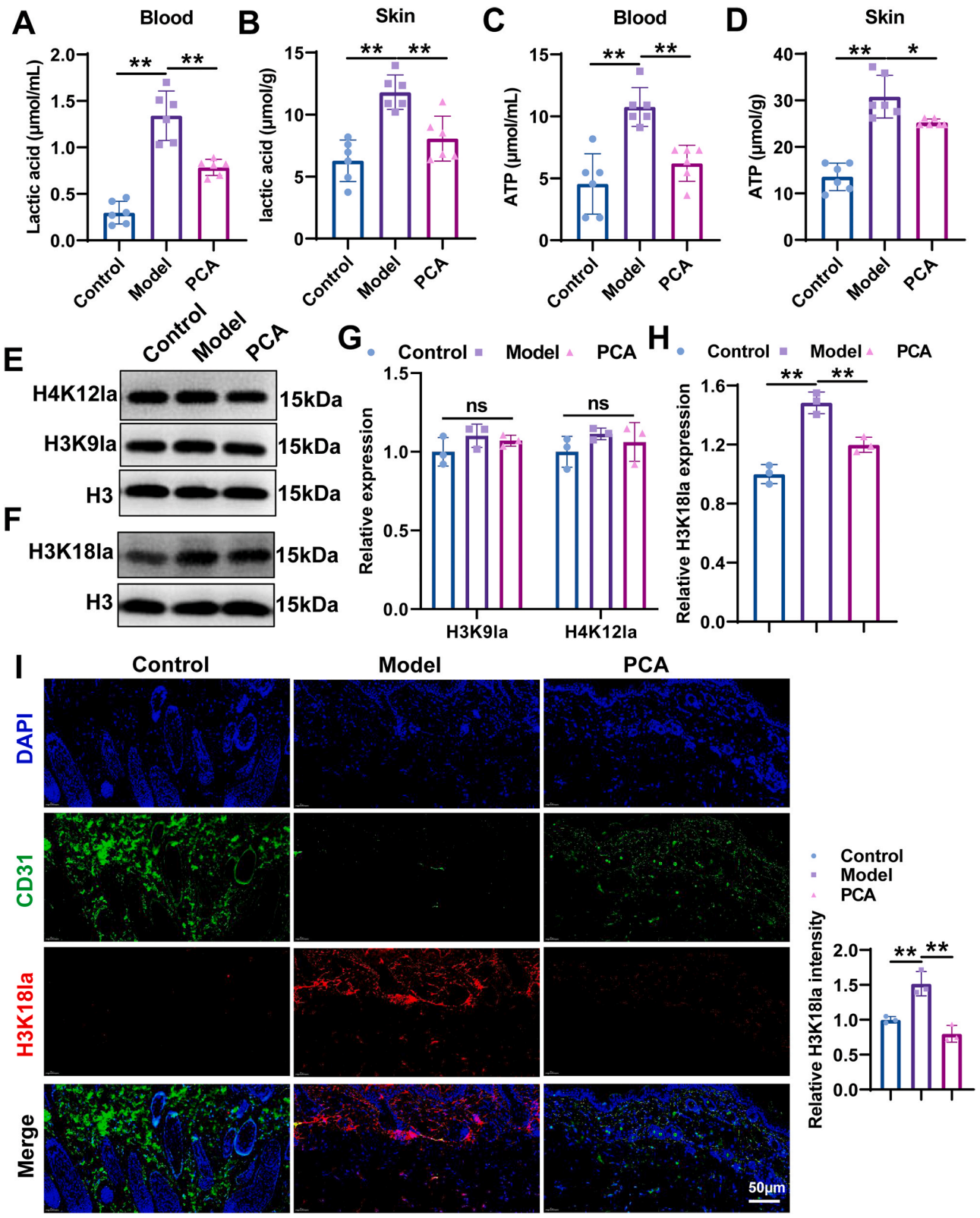

Fig. 3. PCA inhibits histone lactylation of endothelial cells in diabetic wound. (A, B) Effects of PCA on lactic acid levels in blood and skin of model mice. (C, D) Effects of PCA on ATP levels in blood and skin of model mice. (E) Western blot analysis of H4K12la and H3K9la expression in model mice treated with PCA. (F) Western blot analysis of H3K18la expression in model mice treated with PCA. (G) Quantitative analysis of H4K12la and H3K9la expression. (H) Quantitative analysis of H3K18la expression. (I) Immunofluorescence co-staining for CD31 and H3K18la was utilized to detect H3K18la expression in endothelial cells of model mice. ns: no significance. $^{**}p < 0.01$, $^{*}p < 0.05$.

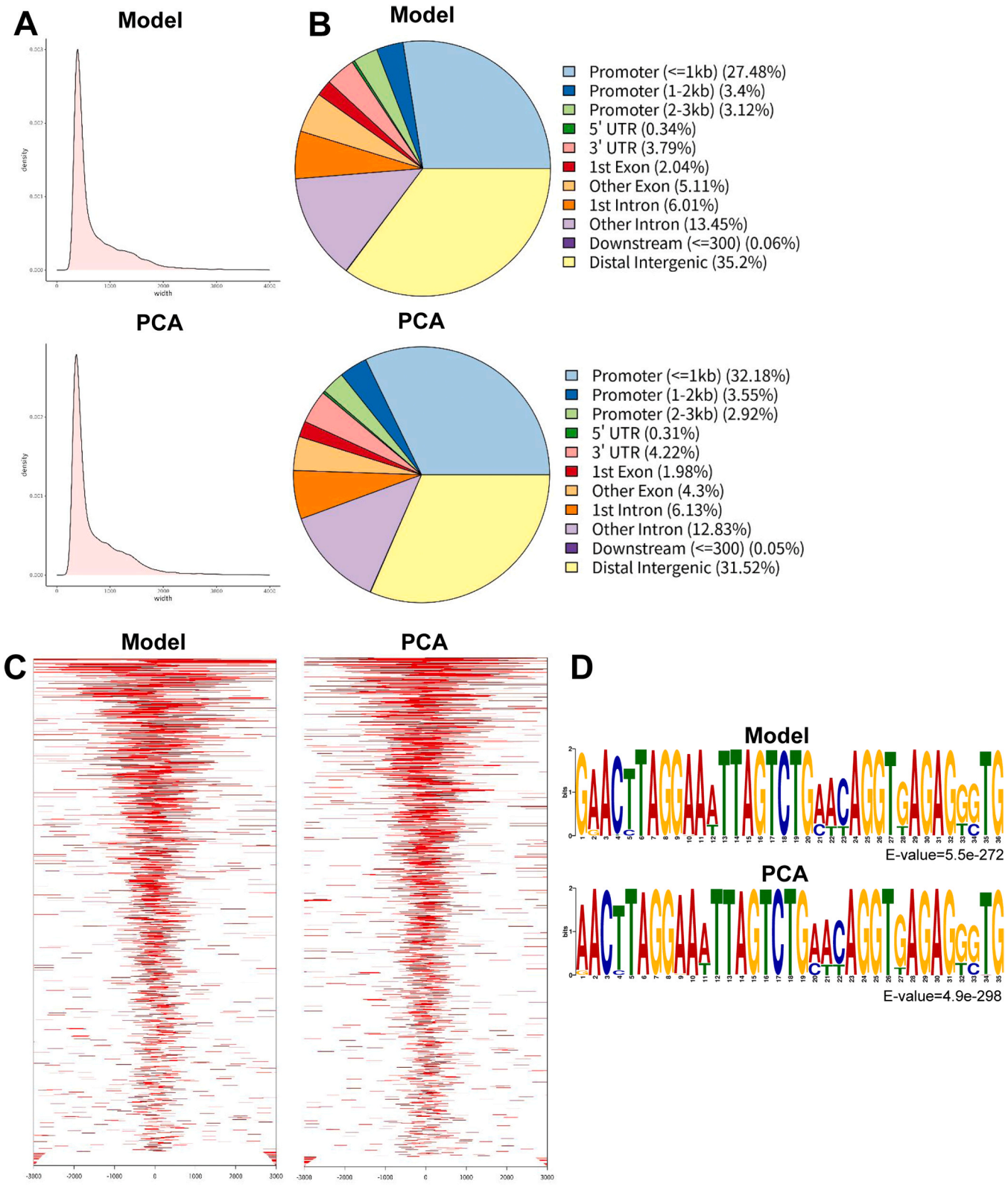

Fig. 4. ChIP-seq analysis of the transcriptional consequences of H3K18la in skin tissues of model and PCA group. (A) Peak annotation analysis was conducted to determine the regions where specific histone modifications occur. (B) Genome-wide distribution of H3K18la-binding peaks. (C) The binding density of H3K18la in skin tissues was visualized by deepTools. (D) Motif analysis was carried out on the sites of H3K18la.

comparable to the effect of rh-bFGF. However, Acvr1c knockdown ameliorated this elevation (Fig. 7E). In the wound healing assay, PCA significantly promoted the migration of HUVECs, an effect comparable to that of rh-bFGF. In contrast, knockdown of Acvr1c markedly reduced HUVEC migration (Fig. 7F, G). The tube formation assay pointed out that Acvr1c knockdown markedly reduced the increased tube formation in PCA-treated HUVECs (Figure S2). Collectively, these results indicated PCA facilitated endothelial angiogenesis via upregulating Acvr1c.

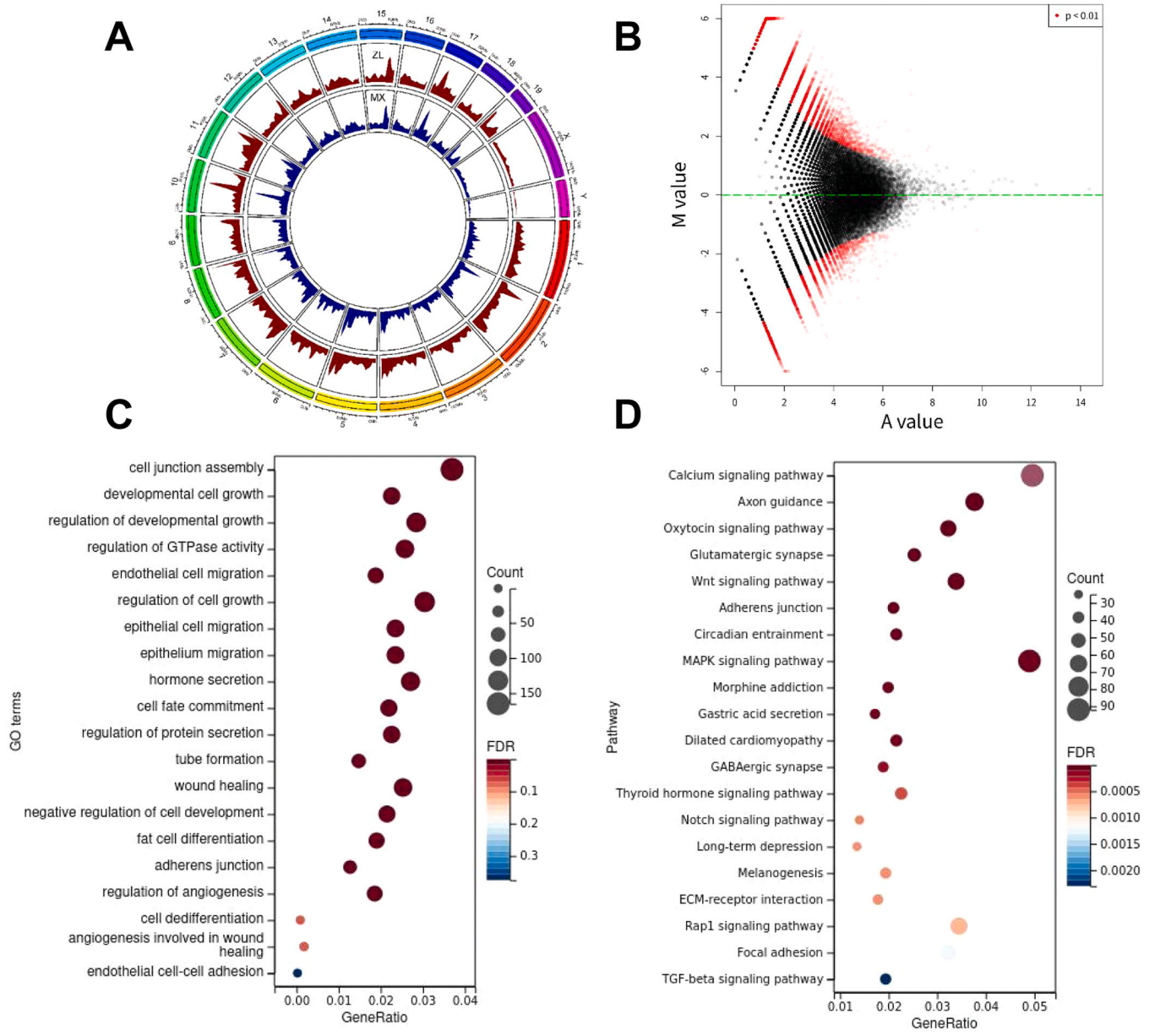

Fig. 5. Analysis of the expression profile of histone lactylation-modified genes in diabetic wound healing. (A) The Circos plot illustrated the distribution of lactylation peaks in the model and PCA groups. (B) The MA plot displayed the changes in differential peaks of H3K18la in the model and PCA groups. (C) GO and (D) KEGG enrichment analysis of H3K18la binding peaks at target genes.

4. Discussion

Diabetic wounds are one of the major complications of diabetes, resulting in a considerable global health care burden (Chen et al., 2022). Diabetic wounds are one of the complications of diabetes and are not easy to heal. Compared to normal wounds, the levels of pro-inflammatory cytokines in diabetic wounds increases, which is not conducive to the normal healing response (Mu et al., 2022). PCA is a natural polyphenol with anti-inflammatory effects (Yang et al., 2021). However, the impact and mechanism of PCA on diabetic wound healing are not yet clear. In this study, we found that PCA treatment significantly facilitated diabetic wound healing, reduced inflammation, and diminished histone lactylation. ChIP-seq analysis revealed that Acvr1c was the target of H3K18la. Mechanistically, PCA inhibited lactate secretion, reduced H3K18la modification, enhanced the expression of Acvr1c, promoted the angiogenesis of HUVECs, thereby facilitating the healing of diabetic wounds (Fig. 8). Our study underscored the promising therapeutic advantages of PCA for promoting wound healing in diabetes.

Although the present study focused on the role of PCA in diabetic wound healing, it is important to note that PCA has also been investigated in other diabetic complications. For instance, PCA suppressed diabetic-induced renal dysfunction and also reduced oxidative stress and inflammation in the kidney of db/db mice (Chang et al., 2021). PCA alleviated oxidative stress in diabetic cataract through GLO1-controlled suppression of AGE/RAGE glycosylation (Cheng et al., 2025). Collectively, these findings suggest that PCA exerts protective effects in diabetic complications. However, to date, there is no direct evidence supporting its role in improving systemic metabolic parameters such as glucose homeostasis or insulin sensitivity. Future studies will be needed to comprehensively evaluate the systemic metabolic effects of PCA to better define its translational potential in diabetes management.

The process of typical wound healing is generally segmented into three stages: the hemostatic-inflammatory, proliferation, and remodeling phases (Wang et al., 2018). Macrophages have been shown to be

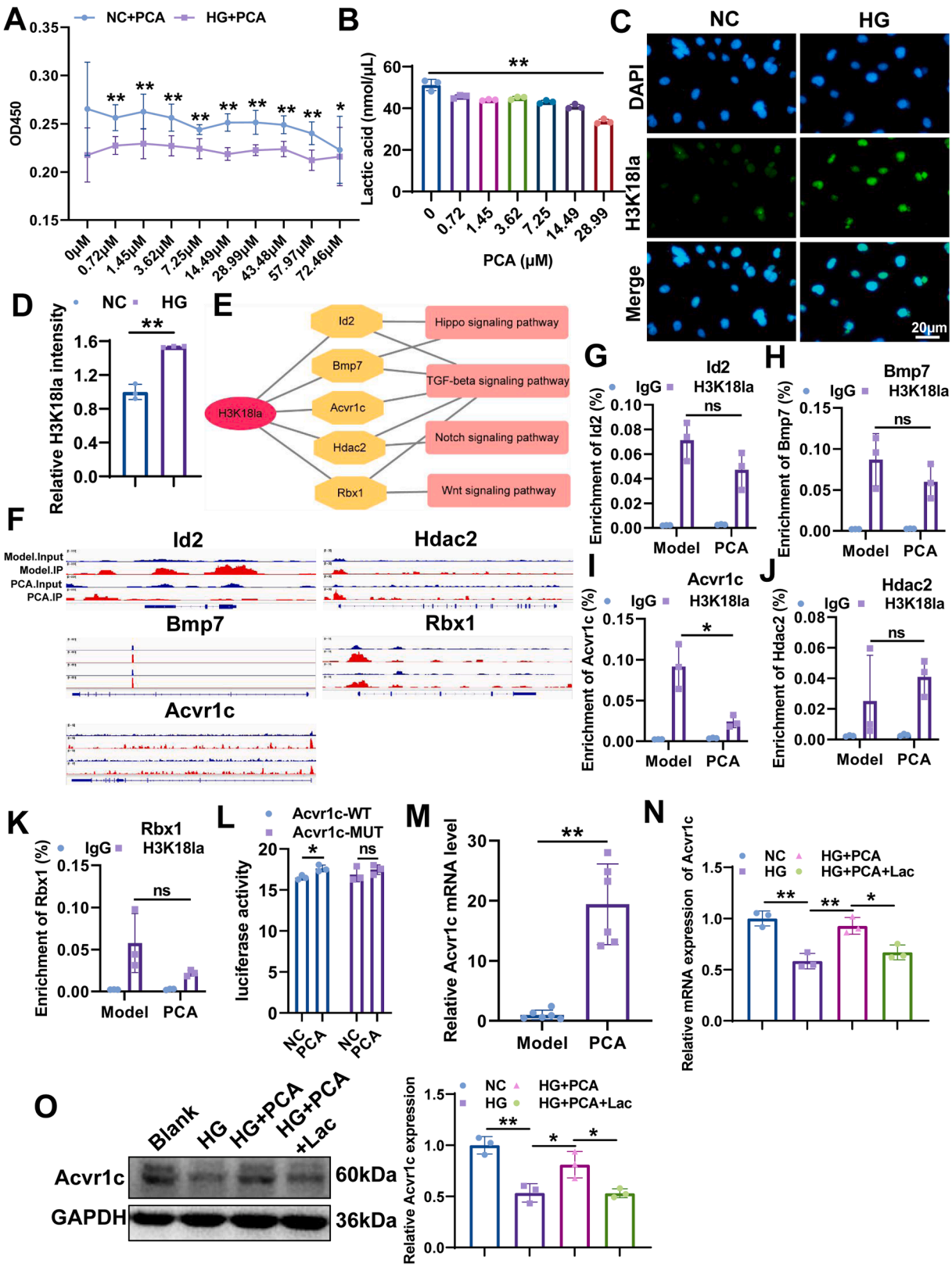

Fig. 6. PCA enhances Acvr1c expression through lactylation. (A) The CCK-8 assay was utilized to detect cell viability of HUVECs treated with high glucose (HG) and different concentrations of PCA (0.72–72.46 μM). (B) Effects of different concentration of PCA on lactic acid in HUVECs. (C) Effects of HG on H3K18la expression in HUVECs were determined by immunofluorescence. (D) Quantitative analysis of H3K18la expression in HUVECs. (E) The network of H3K18la-target genes-angiogenesis-related signaling pathways. (F) The visualization of H3K18la peaks on the five candidate genes. (G-K) ChIP-PCR was used to examine the lactylation of Id2 (G), Bmp7 (H), Acvr1c (I), Hdac2 (J), and Rbx1 (K) in HUVECs. (L) Dual-luciferase reporter assay was carried out to determine the effect of PCA on Acvr1c promoter activity. (M) qRT-PCR was utilized to examine Acvr1c expression in mice wound tissues. (N, O) Effects of PCA and lactic acid on Acvr1c expression were detected by qRT-PCR (N) and western blot (O) in HUVECs. The usage concentration of lactic acid (Lac) was 10 mM. $^{**}p < 0.01$, $^{*}p < 0.05$.

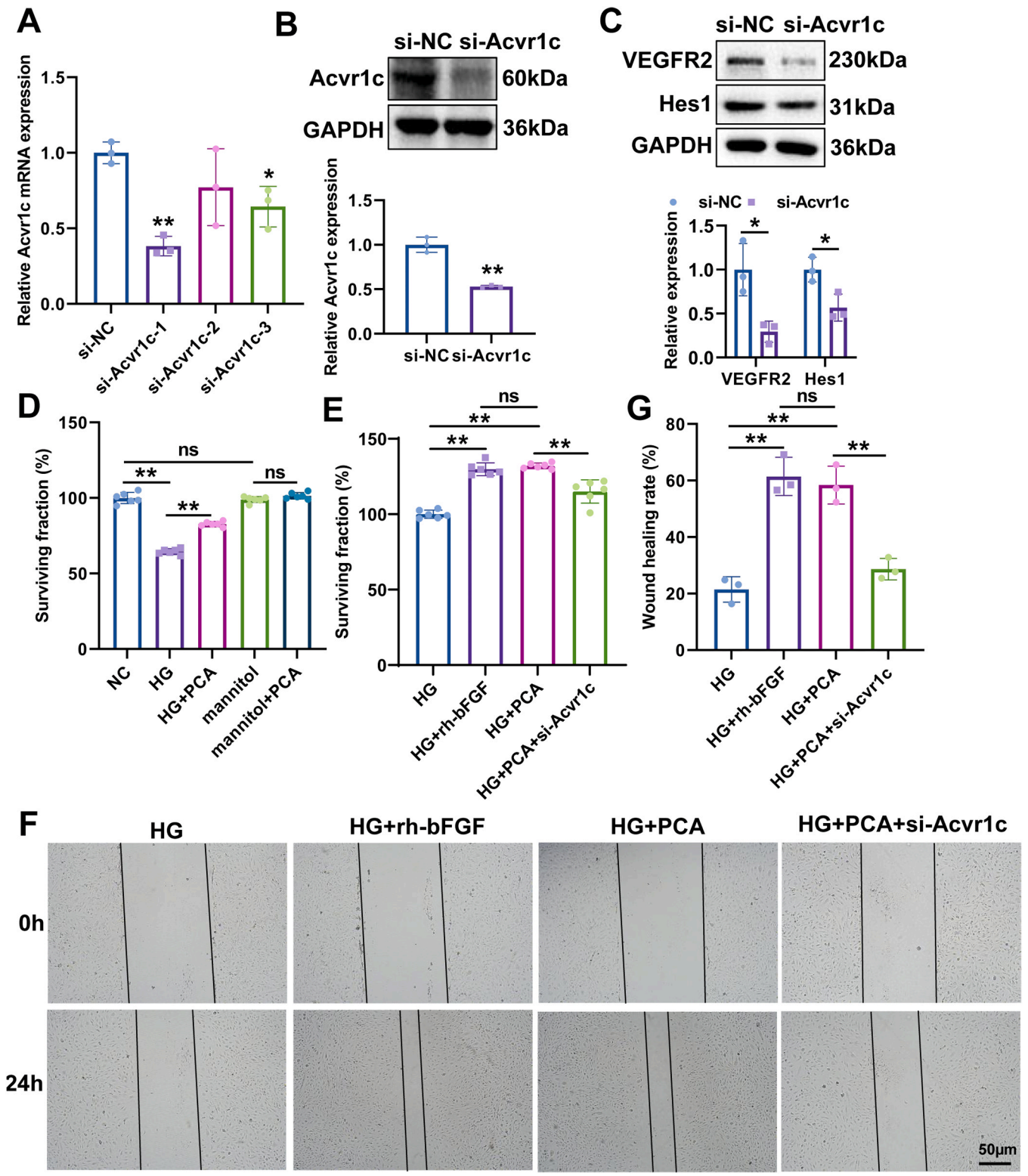

Fig. 7. Acvr1c downregulation reverses PCA-induced angiogenesis of HUVECs. (A) qRT-PCR and (B) western blot were utilized to detect knockdown efficiency of Acvr1c in HUVECs. (C) Western blot analysis of VEGFR2 and Hes1 expression in Acvr1c knockdown HUVECs. (D) The CCK-8 assay was used to evaluate the effect of PCA on HUVEC proliferation. (E) Impacts of Acvr1c downregulation on the proliferation of PCA-treated HUVECs were assessed using the CCK-8 assay. (F) A wound healing assay was used to assess the effect of Acvr1c downregulation on the cell migration of PCA-treated HUVECs. (G) Quantitative analysis of the wound healing assay. $^{**}p < 0.01$, $^{*}p < 0.05$.

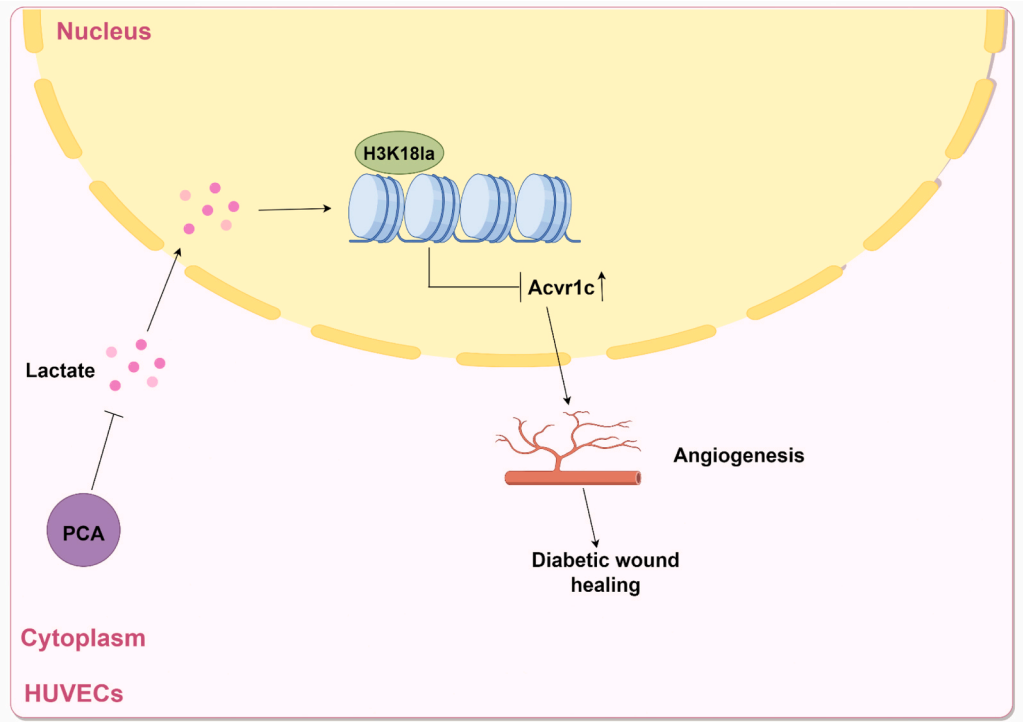

Fig. 8. The proposed model of the mechanism by which PCA promotes diabetic wound healing via histone lactylation.

pivotal during the inflammatory stage of tissue repair (Boniakowski et al., 2017). In diabetic wounds, there is an altered and sustained M1 macrophage phenotype, unlike in normal wounds where a shift to M2 macrophages typically occurs by the third day post-injury (Louiselle et al., 2021). In diabetic mice, resveratrol promoted wound healing by stimulating M2 macrophage polarization (Ding et al., 2022). Apigenin enhanced diabetic wound repair by fostering M2 macrophage polarization through the upregulation of miR-21 (Li et al., 2024b). STING activation by high glucose levels impaired diabetic wound recovery by fostering the M1 polarization of macrophages (Geng et al., 2023). In our study, PCA induced M2 macrophage polarization (CD206 upregulation) and inhibited M1 macrophage polarization (iNOS downregulation) in diabetic mice. Our findings provided a new therapeutic approach for enhancing diabetic wound repair.

Histone lactylation is a recently discovered type of lactate-induced post-translational modification and has garnered considerable attention due to its role in epigenetic regulation (Chen et al., 2021; Li et al., 2022). It has been reported that lactylation modification plays an important role in diabetes-related diseases. For example, histone lactylation H3K18la up-regulated FTO to exacerbate diabetes-induced microvascular dysfunction (Chen et al., 2024). Lactate led to the induction of H3K14la, which promoted epithelial-mesenchymal transition through upregulating KLF5 expression in diabetic kidney disease (Zhang et al., 2024). Suppression of MCT4 counteracted H4K12La in cardiac macrophages and diminished cardiac inflammation in type 2 diabetic mice (Ma et al., 2024). In this study, PCA treatment reversed the elevated lactate levels and H3K18la in diabetic mice.

Recent studies have highlighted diverse molecular strategies for improving diabetic wound repair. For instance, Andersonin-W1 enhanced re-epithelialization and angiogenesis via TLR4/NF-κB signaling, thus promoting diabetic skin wounds (Li et al., 2024a). Cy RL-QN15 expedited wound healing in the scalded dorsal skin of diabetic Kunming mice via interacting with Frizzled-7 receptor (Wu et al., 2024). Peptide-functionalized Fe^{2+}-crosslinked hydrogels have been demonstrated to have promotive effect on infected wounds (Jia et al., 2024). miRNA-365–2–5p was shown to repress SIRT1 expression, thereby boosting injured skin wounds healing (Wei et al., 2025). In our study, PCA enhanced H3K18la-mediated Acvr1c expression and facilitated angiogenesis to promoting wound healing.

In this study, the downstream regulatory mechanism of H3K18la was further explored. Acvr1c was the target of H3K18la and enriched in the TGF-β signaling pathway, which was related with angiogenesis (Liu et al., 2023). We found that PCA inhibited histone lactylation on Acvr1c, leading to an increase in Acvr1c expression. In agreement with our findings, some studies have reported that histone lactylation can inhibit gene transcription. For example, histone lactylation fostered colorectal cancer development via suppressing RARγ transcription (Li et al., 2024c). In pathological pain models such as inflammatory pain, spinal nerve ligation neuropathic pain, chemotherapy-induced neuropathy, and bone cancer pain, lactic acid accumulation drove histone H4K8 lactation, directly inhibiting the transcription of DOCK4 (Xie et al., 2025). In addition, angiogenesis is a crucial process that plays a vital role in diabetic wound healing by offering the necessary oxygen and nutrients to the site of injury (Wang et al., 2024). The TGF-β signaling pathway was reported to function in angiogenesis (Liu et al., 2023). Growth differentiation factor 10 stimulated angiogenesis to facilitating wound healing by triggering the TGF-β1/Smad3 signaling pathway in rats with diabetic foot ulcers (Zhao et al., 2022). Curcumin promotes wound healing by downregulating miR-152–3p and inducing the FBN1/TGF-β pathway in rats with diabetic foot ulcer (Cao et al., 2024). Our study showed that Acvr1c knockdown reversed the PCA-induced increased angiogenesis in HUVECs, indicating PCA expedites diabetic wound healing via Acvr1c-mediated angiogenesis.

There were several limitations in this study. First, although the diabetic wound mouse model provided valuable insights into the role of PCA in vivo, it cannot fully replicate the complex pathological and physiological processes of human diabetic wound healing. Therefore, further validation in larger animal models and clinical samples is required. Second, future research needs to apply direct observation methods such as fluorescence labeling to clarify the uptake process of PCA. Third, this study mainly focused on the role of H3K18la and Acvr1c in mediating the effects of PCA. However, histone lactylation may regulate multiple downstream genes and pathways involved in angiogenesis and tissue repair, which were not comprehensively investigated.

Finally, the study only used a single administration route to verify the efficacy in a diabetic mouse model, without comparing the bioavailability and efficacy differences of other common administration methods.

In conclusion, our findings suggest that PCA inhibited lactate secretion, leading to a decrease in H3K18la, which promotes Acvr1c expression, consequently resulting in angiogenesis and ultimately promoting diabetic wound healing. Our results indicate that PCA could be a viable approach for enhancing diabetic wound repair through histone lactylation.

CRediT authorship contribution statement

Yin Qu: Supervision, Conceptualization. **Yang You:** Writing – original draft, Project administration, Methodology, Data curation, Writing – review & editing. **Weijing Fan:** Writing – original draft, Project administration, Methodology, Data curation, Writing – review & editing. **Guobin Liu:** Supervision, Conceptualization.

Ethics approval

This study was approved by the Ethical Committee of Shuguang Hospital Affiliated to Shanghai University of Traditional Chinese Medicine.

Funding

This work was supported by National Natural Science Foundation of China (82104868), State Administration of Traditional Chinese Medicine's seventh batch of academic experience inheritance projects for national veteran Chinese medicine experts [National Chinese Medicine Medical People's Education Letter (2022) No. 76], Shanghai Traditional Chinese Medicine University Affiliated Hospital "Clinical Research Key Talents Training Plan" (2023LCRC07), Shanghai 2024 Annual "Science and Technology Innovation Action Plan" Rising Star Project Application Guidelines/Rising Star Cultivation (24YF2746800), Shanghai University of Traditional Chinese Medicine Affiliated Shuguang Hospital Siming Fund (SGKJ-202301), Shanghai Municipal Health Commission's Special Project for Clinical Research in the Health Industry (20234Y0162).

Declaration of Competing Interest

All authors declare that they have no conflict of interest.

Acknowledgments

We are grateful to MivectorBio Biotechnology for assisting in sequencing and bioinformatics analysis.

Appendix A. Supporting information

Supplementary data associated with this article can be found in the online version at doi:10.1016/j.molimm.2025.09.002.

Data availability

Data will be made available on request.

References

Boniakowski, A.E., Kimball, A.S., Jacobs, B.N., Kunkel, S.L., Gallagher, K.A., 2017. Macrophage-Mediated inflammation in normal and diabetic wound healing. J. Immunol. 199, 17–24.

Burgess, J.L., Wyant, W.A., Abdo Abujamra, B., Kirsner, R.S., Jozic, I., 2021. Diabetic Wound-Healing science. Medicina 57.

Cao, M., Duan, Z., Wang, X., Gong, P., Zhang, L., Ruan, B., 2024. Curcumin promotes diabetic foot ulcer wound healing by inhibiting miR-152-3p and activating the FBN1/TGF-beta pathway. Mol. Biotechnol. 66, 1266–1278.

Chang, M., Nguyen, T.T., 2021. Strategy for treatment of infected diabetic foot ulcers. Acc. Chem. Res. 54, 1080–1093.

Chang, Y.T., Chung, M.C., Hsieh, C.C., Shieh, J.J., Wu, M.J., 2021. Evaluation of the therapeutic effects of protocatechuic aldehyde in diabetic nephropathy. Toxins 13.

Chen, A.N., Luo, Y., Yang, Y.H., Fu, J.T., Geng, X.M., Shi, J.P., Yang, J., 2021. Lactylation, a novel metabolic reprogramming code: current status and prospects. Front. Immunol. 12, 688910.

Chen, G.Y., Wang, L.Z., Cui, Y., Liu, J.C., Wang, L.Q., Wang, L.L., Sun, J.Y., Liu, C., Tan, H.L., Li, Q., Jin, Y.S., Xu, Z.C., Yu, D.J., 2022. Serum metabolomic analysis reveals key metabolites in drug treatment of central precocious puberty in female children. Front. Mol. Neurosci. 15, 972297.

Chen, X., Wang, Y., Wang, J.N., Zhang, Y.C., Zhang, Y.R., Sun, R.X., Qin, B., Dai, Y.X., Zhu, H.J., Zhao, J.X., Zhang, W.W., Ji, J.D., Yuan, S.T., Shen, Q.D., Liu, Q.H., 2024. Lactylation-driven FTO targets CDK2 to aggravate microvascular anomalies in diabetic retinopathy. EMBO Mol. Med. 16, 294–318.

Cheng, X., Zhao, S., Chen, Y., Wang, J., Han, F., 2025. Protocatechualdehyde attenuates oxidative stress in diabetic cataract via GLO1-mediated inhibition of AGE/RAGE glycosylation. Front. Pharmacol. 16, 1586173.

Defeudis, G., Mazzilli, R., Tenuta, M., Rossini, G., Zamponi, V., Olana, S., Faggiano, A., Pozzilli, P., Isidori, A.M., Gianfrilli, D., 2022. Erectile dysfunction and diabetes: a melting pot of circumstances and treatments. Diabetes/Metab. Res. Rev. 38, e3494.

Deng, L., Du, C., Song, P., Chen, T., Rui, S., Armstrong, D.G., Deng, W., 2021. The role of oxidative stress and antioxidants in diabetic wound healing. Oxid. Med. Cell. Longev. 2021, 8852759.

Ding, Y., Yang, P., Li, S., Zhang, H., Ding, X., Tan, Q., 2022. Resveratrol accelerates wound healing by inducing M2 macrophage polarisation in diabetic mice. Pharm. Biol. 60, 2328–2337.

Fan, H., Yang, F., Xiao, Z., Luo, H., Chen, H., Chen, Z., Liu, Q., Xiao, Y., 2023. Lactylation: novel epigenetic regulatory and therapeutic opportunities. Am. J. Physiol. Endocrinol. Metab. 324, E330–E338.

Fang, X., Liu, Y., Lu, J., Hong, H., Yuan, J., Zhang, Y., Wang, P., Liu, P., Ye, J., 2018. Protocatechuic aldehyde protects against isoproterenol-induced cardiac hypertrophy via inhibition of the JAK2/STAT3 signaling pathway. NaunynSchmiede 's. Arch. Pharmacol. 391, 1373–1385.

Gao, L., Wu, W.F., Dong, L., Ren, G.L., Li, H.D., Yang, Q., Li, X.F., Xu, T., Li, Z., Wu, B.M., Ma, T.T., Huang, C., Huang, Y., Zhang, L., Lv, X., Li, J., Meng, X.M., 2016. Protocatechuic aldehyde attenuates Cisplatin-Induced acute kidney injury by suppressing Nox-Mediated oxidative stress and renal inflammation. Front. Pharmacol. 7, 479.

Geng, K., Ma, X., Jiang, Z., Huang, W., Gu, J., Wang, P., Luo, L., Xu, Y., Xu, Y., 2023. High glucose-induced STING activation inhibits diabetic wound healing through promoting M1 polarization of macrophages. Cell death Discov. 9, 136.

Huang, X., Yip, K., Nie, H., Chen, R., Wang, X., Wang, Y., Lin, W., Li, R., 2024. ChIP-seq and RNA-seq reveal the involvement of histone lactylation modification in gestational diabetes mellitus. J. Proteome Res. 23, 1937–1947.

Huang, Z., Huang, S., Song, T., Yin, Y., Tan, C., 2021. Placental angiogenesis in mammals: a review of the regulatory effects of signaling pathways and functional nutrients. Adv. Nutr. 12, 2415–2434.

Ji, B., Yuan, K., Li, J., Ku, B.J., Leung, P.S., He, W., 2021. Protocatechualdehyde restores endothelial dysfunction in streptozotocin-induced diabetic rats. Ann. Transl. Med. 9, 711.

Jia, Q., Fu, Z., Li, Y., Kang, Z., Wu, Y., Ru, Z., Peng, Y., Huang, Y., Luo, Y., Li, W., Hu, Y., Sun, X., Wang, J., Deng, Z., Wu, C., Wang, Y., Yang, X., 2024. Hydrogel loaded with Peptide-Containing nanocomplexes: symphonic cooperation of photothermal antimicrobial nanoparticles and prohealing peptides for the treatment of infected wounds. ACS Appl. Mater. Interfaces 16, 13422–13438.

Kim, K.J., Kim, M.A., Jung, J.H., 2008. Antitumor and antioxidant activity of protocatechualdehyde produced from streptomyces lincolnensis M-20. Arch. pharmacal Res. 31, 1572–1577.

Li, C., Xiong, Y., Fu, Z., Ji, Y., Yan, J., Kong, Y., Peng, Y., Ru, Z., Huang, Y., Li, Y., Yang, Y., He, L., Tang, J., Wang, Y., Yang, X., 2024a. The direct binding of bioactive peptide Andersonin-W1 to TLR4 expedites the healing of diabetic skin wounds. Cell. Mol. Biol. Lett. 29, 24.

Li, K., Wu, L., Jiang, J., 2024b. Apigenin accelerates wound healing in diabetic mice by promoting macrophage M2-type polarization via increasing miR-21 expression. Mol. Cell. Biochem. 479, 3119–3127.

Li, X., Yang, Y., Zhang, B., Lin, X., Fu, X., An, Y., Zou, Y., Wang, J.X., Wang, Z., Yu, T., 2022. Lactate metabolism in human health and disease. Signal Transduct. Target. Ther. 7, 305.

Li, X.M., Yang, Y., Jiang, F.Q., Hu, G., Wan, S., Yan, W.Y., He, X.S., Xiao, F., Yang, X.M., Guo, X., Lu, J.H., Yang, X.Q., Chen, J.J., Ye, W.L., Liu, Y., He, K., Duan, H.X., Zhou, Y.J., Gan, W.J., Liu, F., Wu, H., 2024c. Histone lactylation inhibits RARgamma expression in macrophages to promote colorectal tumorigenesis through activation of TRAF6-IL-6-STAT3 signaling. Cell Rep. 43, 113688.

Lin, J., Ren, J., 2024. Lactate-induced lactylation and cardiometabolic diseases: from epigenetic regulation to therapeutics. Biochim. Et. Biophys. Acta Mol. basis Dis. 1870, 167247.

Liu, H., Sun, M., Wu, N., Liu, B., Liu, Q., Fan, X., 2023. TGF-beta/Smads signaling pathway, Hippo-YAP/TAZ signaling pathway, and VEGF: their mechanisms and roles in vascular remodeling related diseases. Immun. Inflamm. Dis. 11, e1060.

Louiselle, A.E., Niemiec, S.M., Zgheib, C., Liechty, K.W., 2021. Macrophage polarization and diabetic wound healing. Transl. Res. J. Lab. Clin. Med. 236, 109–116.

Ma, X.M., Geng, K., Wang, P., Jiang, Z., Law, B.Y., Xu, Y., 2024. MCT4-dependent lactate transport: a novel mechanism for cardiac energy metabolism injury and inflammation in type 2 diabetes mellitus. Cardiovasc. Diabetol. 23, 96.
Mu, X., Wu, X., He, W., Liu, Y., Wu, F., Nie, X., 2022. Pyroptosis and inflammasomes in diabetic wound healing. Front. Endocrinol. 13, 950798.
Okonkwo, U.A., DiPietro, L.A., 2017. Diabetes and wound angiogenesis. Int. J. Mol. Sci. 18.
Tousian, H., Razavi, B.M., Hosseinzadeh, H., 2020. Effects of alpha-mangostin on memory senescence induced by high glucose in human umbilical vein endothelial cells. Iran. J. Basic Med. Sci. 23, 1261–1267.
Wang, P.H., Huang, B.S., Horng, H.C., Yeh, C.C., Chen, Y.J., 2018. Wound healing. J. Chin. Med. Assoc. JCMA 81, 94–101.
Wang, X., Li, R., Zhao, H., 2024. Enhancing angiogenesis: Innovative drug delivery systems to facilitate diabetic wound healing. Biomedicine & pharmacotherapy = Biomedecine & pharmacotherapie 170, 116035.
Wei, G., Guan, Y., Yin, Y., Duan, J., Zhou, D., Zhu, Y., Quan, W., Xi, M., Wen, A., 2013. Anti-inflammatory effect of protocatechuic aldehyde on myocardial ischemia/reperfusion injury in vivo and in vitro. Inflammation 36, 592–602.
Wei, Z., Li, X., Zhou, J., Zhou, Y., Xiao, Z., Yang, Q., Liu, X., Peng, Y., Yang, Y., Ding, Y., Ru, Z., Wang, Y., Yang, M., Yang, X., 2025. Inhibition of miRNA-365-2-5p targeting SIRT1 regulates functions of keratinocytes to enhance wound healing. FASEB J. Off. Publ. Fed. Am. Soc. Exp. Biol. 39, e70560.
Wu, Y.T., Ru, Z.Q., Peng, Y., Fu, Z., Jia, Q.Y., Kang, Z.J., Li, Y.S., Huang, Y.B., Yin, S.G., Guo, K., Liu, N.X., Feng, C.A., Tang, J., Zhang, B.Y., Yang, Z., Wang, Y., Yang, X.W., 2024. Peptide cy (RL-QN15) accelerates hair regeneration in diabetic mice by binding to the Frizzled-7 receptor. Zool. Res. 45, 1287–1299.
Xie, M.X., Lai, R.C., Xiao, Y.B., Zuo, S.Y., Tang, H., Cao, X.Y., Liu, J.K., Zhou, Z.S., Wang, S.H., Lu, X.F., He, Y., Xie, Y., Zhang, X.L., 2025. Histone lactylation regulates DOCK4 to control heat nociception and supports Dynein-mediated Nav1.7 trafficking. Nat. Commun. 16, 7165.
Xie, Y., Hu, H., Liu, M., Zhou, T., Cheng, X., Huang, W., Cao, L., 2022. The role and mechanism of histone lactylation in health and diseases. Front. Genet. 13, 949252.
Yang, J., Li, J., Tan, R., He, X., Lin, X., Zhong, X., Fan, J., Wang, L., 2021. Protocatechualdehyde attenuates obstructive nephropathy through inhibiting lncRNA9884 induced inflammation. Phytother. Res. PTR 35, 1521–1533.
Yang, Y., Song, L., Yu, L., Zhang, J., Zhang, B., 2025. H4K12 lactylation potentiates mitochondrial oxidative stress via the Foxo1 pathway in diabetes-induced cognitive impairment. J. Adv. Res.
Zhang, D., Tang, Z., Huang, H., Zhou, G., Cui, C., Weng, Y., Liu, W., Kim, S., Lee, S., Perez-Neut, M., Ding, J., Czyz, D., Hu, R., Ye, Z., He, M., Zheng, Y.G., Shuman, H.A., Dai, L., Ren, B., Roeder, R.G., Becker, L., Zhao, Y., 2019. Metabolic regulation of gene expression by histone lactylation. Nature 574, 575–580.
Zhang, X., Chen, J., Lin, R., Huang, Y., Wang, Z., Xu, S., Wang, L., Chen, F., Zhang, J., Pan, K., Yin, Z., 2024. Lactate drives epithelial-mesenchymal transition in diabetic kidney disease via the H3K14la/KLF5 pathway. Redox Biol. 75, 103246.
Zhang, Y., Wang, D., Zhao, Z., Liu, L., Xia, G., Ye, T., Chen, Y., Xu, C., Jin, X., Shen, C., 2022. Nephronectin promotes cardiac repair post myocardial infarction via activating EGFR/JAK2/STAT3 pathway. Int. J. Med. Sci. 19, 878–892.
Zhao, Q., Xu, J., Han, X., Zhang, Z., Qu, J., Cheng, Z., 2022. Growth differentiation factor 10 induces angiogenesis to promote wound healing in rats with diabetic foot ulcers by activating TGF-beta1/Smad3 signaling pathway. Front. Endocrinol. 13, 1013018.
Zheng, Y., Ley, S.H., Hu, F.B., 2018. Global aetiology and epidemiology of type 2 diabetes mellitus and its complications. Nat. Rev. Endocrinol. 14, 88–98.